The final publication is available at

https://doi.org/10.1016/j.compstruct.2018.05.076

Additional Information

RELEVANT FACTORS IN THE DESIGN OF COMPOSITE BALLISTIC HELMETS

Marta Palomar[1], Estívaliz Lozano-Mínguez[1], Marcos Rodríguez-Millán[2], María Henar Miguélez[2], Eugenio Giner[1*]

[1] *Centre of Research on Mechanical Engineering-CIIM, Department of Mechanical Engineering and Materials, Universitat Politècnica de València, Camino de Vera s/n, 46022 Valencia, Spain*
[2] *Department of Mechanical Engineering, Universidad Carlos III de Madrid, Avda. de la Universidad 30, 28911, Leganés (Madrid), Spain*
*Corresponding author (eginerm@mcm.upv.es)

ABSTRACT

In this paper, the design methodology of composite ballistic helmets has been enhanced considering biomechanical requirements by means of finite element analysis. Modern combat helmets lead to a new type of non-penetrating injury, the Behind Helmet Blunt Trauma (BHBT), generated by the deformation of the inner face of the helmet, the so-called backface deformation (BFD). Current standard testing methodologies use BFD as the main measure in ballistic testing. Nonetheless, this work discusses the relationship between this mechanical parameter and the head trauma (BHBT) by studying different head injury criteria. A numerical model consisting of a helmet and a human head is developed and validated with experimental data from literature. The consequences of non-penetrating high-speed ballistic impacts upon the human head protected by an aramid combat helmet are analysed, concluding that the existing testing methodologies fail to predict many types of head injuries. The influence of other parameters like bullet velocity or head dimensions is analysed. Usually, a single-sized helmet shell is manufactured and the different sizes are adjusted by varying the foam pad thickness. However, one of the conclusions of this work is that pad thickness is critical to avoid BHBT and must be considered in the design process.

Key words: Combat helmet design; ballistic standards; human head model; head injury criteria

Abbreviations	
ACH	Advanced Combat Helmet
BFD	Back Face Deformation
BHBT	Behind Helmet Blunt Trauma
BPT	Brain Pressure Tolerance
CSDM	Cumulative Strain Damage Measure
CSF	Cerebrospinal Fluid
CT	Computed Tomography
DAI	Diffuse Axonal Injury
DDM	Dilatation Damage Measure
FE	Finite Element
FMJ	Full Metal Jacket
HIC	Head Injury Criterion
ICP	Intracranial Pressure
PASGT	Personnel Armour System Ground Troops
PMHS	Post-Mortem Human Specimen

SFC	Skull Fracture Correlate
TBI	Traumatic Brain Injury
UHMWPE	Ultra-High Molecular Weight Polyethylene

1. INTRODUCTION

In the current context of military conflicts and terrorism activities, ballistic head injuries entail a health problem of increasing relevance affecting both civilian and military population [1]. Concerning ballistic protections, many attempts have been made over the last decades to improve the effectiveness of combat helmets. Heavy metallic helmets have been replaced by composite shells, which offer better strength-to-weight ratios. Despite the increased penetration resistance, the occurrence of large deformations increases the probability of Behind Helmet Blunt Trauma (BHBT). This is a non-penetrating injury caused by the strike of the inner surface of the helmet to the head [2–4], quantified through the measurement of the Back Face Deformation (BFD) [5]. The consequences of excessive BFD range from mild injuries in the cranium and brain to irreversible trauma and skull fracture.

The role of personal protective equipment (combat helmet) is crucial in order to minimize the morbidity and mortality resulting from ballistic head injuries. In ballistic standards, the maximum allowable BFD for combat helmets is established in terms of rear effect, which is usually evaluated on ballistic clay. It is clear that the internal head damage caused by the impact wave cannot be assessed in current standards through the evaluation of the deformation left in the clay.

This paper focuses on BHBT analysis with the aim of improving combat helmet design accounting for biomechanical considerations. Main contributions in the literature regarding experiments and numerical modeling of BHBT modeling are summarized in this section, including an overview of head injury criteria.

1.1. *Experimental work focusing on BHBT*

Traditionally, experimental testing concerning ballistic induced injuries have been limited to animal tests and postmortem human head/neck specimens due to moral considerations and set-up complexity. Experimental ballistic tests on helmeted heads and headforms have been carried out recently by [6–8] to assess BHBT. Experiments by Sarron et al. [6] were based on 9 mm calibre bullets impacting fresh human cadaver heads and human dry skulls protected by plates of different materials, which were placed at a certain distance from the subject. The projectile velocity was about 400 m/s and the impact site was the parietal region of the head. They highlighted the strong influence of the protective material properties and the distance between the plate and the head/skull on skull fracture and brain injury. They stated that a distance of 11-12 mm was sufficient to prevent skull fracture and to decrease intracranial pressures to low-risk injury values. Based on the results obtained by Bass et al. [9] they proposed a contact pressure threshold of 50-100 MPa for the occurrence of skull fracture.

Rafaels et al. [8] conducted ballistic tests on seven helmeted post-mortem human specimen (PMHS). The helmet was based on ultra-high molecular weight polyethylene (UHMWPE) presenting large deformations under ballistic impact. They used 9 mm bullets with velocities ranging between 404.9 and 459 m/s. Moderate-velocity tests (440-445 m/s) resulted in linear skull fractures (a fracture pattern with a single or few cracks as opposed to comminuted fractures) at different locations and depressed fracture at the impact site. Higher velocities

showed linear fractures close to the left temporal region (impact region). Bass et al. [10] developed an injury risk curve from these data as a function of muzzle velocity.

Freitas et al. [7] constructed a human head surrogate using refreshed skulls and synthetic materials to represent the most relevant soft tissues in the human head. They performed ballistic tests upon this surrogate wearing a Lightweight Combat Helmet (LWH) using different ammunition and helmet internal padding configurations. For 9 mm full metal jacket (FMJ) bullets at an average speed of 438 m/s, moderate cranial fractures occurred in the cases where the frontal foam pads had been removed. On the contrary, under the same loading conditions no injury was found when the cushioning of the helmet was complete, thus highlighting the importance of using proper inner protections.

Despite providing useful tangible information on skull fracture, experimental ballistic tests on such surrogate heads have limitations to faithfully represent the impact response of soft human tissues. Head surrogates offer more a qualitative rather than a quantitative approach of closed head injury, as most or all living tissues are replaced by synthetic materials. Besides, post mortem specimens do not match the actual response of living organs, since their properties are altered by the cease of blood flow.

1.2. *Numerical modelling of BHBT*

In addition to experimental testing, numerical modelling may provide a helpful design tool for combat helmets, allowing the fulfillment of standards requirements and the characterization of the physics of the problem in terms of relevant mechanical variables such as stress, strain, and acceleration. The design objectives include, among others, reducing the BFD effect, and the aiding of material selection for strength and possible weight reduction so as to improve protection from blunt trauma and ergonomics.

The limitations and complexity of experiments have led to recent finite element (FE) based studies on biomechanics of ballistic impact [11–13]. Aare et al. [11] performed ballistic impact simulations using a FE helmet model based on a Personnel Armour System Ground Troops (PASGT) geometry and a numerical head model developed by Kleiven et al. [14] and validated against PMHS experimental test data. The bullet was modelled as a rigid body with a weight of 8 g with shot velocity 360 m/s. They studied the influence of both helmet shell stiffness and bullet impact angle on the kinematic and mechanical behaviour of the different head tissues. Stiffer shell configurations led to lower stresses in cranial bone due to the diminished contact between the head and the helmet, but tended to increase the strains in the brain. Regarding the impact angle, when the bullet was perpendicular to the helmet surface the greatest skull stresses were reached, whereas oblique directions brought about an increase of shear strains in the brain.

Numerical simulations of the helmet testing procedures defined in the National Institute of Justice (NIJ) standard [15] were conducted by Li et al. [12]. The authors modelled an Advanced Combat Helmet (ACH) consisting of twelve-layer Kevlar and coupled on a dummy/clay headform. NIJ conditions for frontal and lateral impacts were simulated by Li et al. [13] to analyse BHBT on a FE human head model developed by the Royal Institute of Technology (KTH) in Sweden [16]. The protection was an ACH with two different padding materials in the interior cushioning, and the projectile was a 9 mm FMJ. The effects of the padding material stiffness, stand-off distance, helmet thickness and bullet incidence angle on the resulting head injury were studied. They concluded that the use of soft padding decreases both the risk of skull fracture and the maximum strains and stresses in the brain, whereas stiff foams can have similar effects as the helmet without padding.

3

1.3. *Head injury criteria*

Extensive research has been made in other fields (such as sport science involving impact contacts and in the automotive sector for crash accidents) in the prevention of Traumatic Brain Injury (TBI) through the proper design of protections accounting for biomechanical effects, see for instance [17–19]. However, the validity of the currently developed head injury criteria in ballistics is still being debated. Some of the most representative head injury criteria concerning skull fracture and brain injury are summarized in Table 1 and briefly discussed in the following paragraphs.

Table 1.
Head injury criteria from the literature studied in this work.

		Critical values
Skull Fracture	**Acceleration criteria**	
	HIC_{15}	700 -> 31% of fracture probability [20]
	Skull Fracture Correlate (SFC)	120 g -> 15% of fracture probability [21]
	Hertz probability of fracture	Measured as the calculated probability [22]
	Principal stresses	
	Compact bone	90, -132 MPa [23]
	Diplöe	34.8, -24.8 MPa [23]
Brain Injury	**Strain**	
	Cumulative Strain Damage Measure (CSDM)	55% -> 50% probability of concussion for a ε_{crit} of 0.15 [24]
	Pressure	
	Dilatation Damage Measure (DDM)	7.2% -> 50% probability of contusions [24]
	Intracranial pressure	234 kPa [25] -> severe injury

- *Skull fracture*

One of the first criteria to assess head injury is the *Head Injury Criterion* (HIC). It was developed in 1972 for the automotive applications, and takes into account the translational acceleration history $a(t)$ integrated along a time domain limited by instants t_1 and t_2 maximizing Equation 1:

$$HIC = \left\{ \left[\frac{1}{t_2-t_1} \int_{t_1}^{t_2} a(t)dt \right]^{2.5} (t_2 - t_1) \right\}_{max} \qquad (1)$$

Despite HIC being still currently used at present, this criterion lacks the rotational kinematics contribution, thus making it unable to predict many injury mechanisms [21]. For high-speed events such as ballistic impacts, peak accelerations are reached at a short time (approximately 1 ms) and involve great energy transfer in comparison to those situations for which HIC was intended, such as the automotive accidents [10].

Modifications of this criterion have been developed in later works. In 1993, Hertz [22] proposed a probability curve for skull fracture based on cadaveric experiments. In this work, the

probability of skull fracture is estimated as a cumulative function of a lognormal distribution of HIC given in Equation 2.

$$p\,(fract) = N\left(\frac{\ln HIC - \mu}{\sigma}\right) \tag{2}$$

Ruan et al. [26] studied the influence of the skull thickness on the response under impact conditions. The analysis regarded the probability of skull fracture in terms of HIC, and compiled the fracture risk curves that had been proposed in literature up to that moment: Hertz [22], Mertz et al. [27], and Prasad and Mertz [28]. The lognormal probability function proposed by Hertz [22] was found to be the most restrictive, setting the 50%-probability of fracture for the value 1150 HIC whilst the other curves set this probability for the range 1450-1550 HIC.

In 2003, Vorst et al. [21] took the results from the experimental tests on PMHS carried out by Hodgson and Thomas [29] and performed regression analyses to study the correlation between linear skull fracture and other parameters, including HIC. In this work, the Skull Fracture Correlate (SFC) defined in Equation 3 was considered optimal for skull fracture prediction:

$$SFC = \frac{\Delta V_{HIC}}{\Delta T_{HIC}} = \frac{\int_{t_1}^{t_2} a(t)dt}{(t_2 - t_1)} \tag{3}$$

This predictor correlates with skull strain under impact loading conditions and is considered the most suitable for the assessment of frontal crash accidents. The value of SFC equal to 120 g corresponds to 15% probability of skull fracture.

Lately, Sahoo et al. [23] reconstructed several real trauma cases by means of FE and developed skull fracture risk curves as a function of force, SFC, HIC and internal skull energy, respectively. They concluded that internal skull energy was statistically the most suitable parameter to predict skull fracture, and proposed a threshold of 453 mJ for 50% of fracture risk.

- ***Brain Injury***

Regarding the trauma suffered by the brain tissue when subjected to impact loading, two main injury types can be distinguished: diffuse and focal. Diffuse injuries appear to be the most common manifestation of TBI in non-penetrating ballistic impacts because of the load distribution in the helmet shell and the padding system [30] which may vary within helmet types. Diffuse Axonal Injury (DAI) ranges from mild (concussion) to severe [31,32] and the transition thresholds between those injury levels are not clearly defined. Margulies et al. [32] collected experimental data of induced rotations on the heads of anesthetized baboons until coma was achieved. They proposed a critical shear strain value in the brain of 0.05 for moderate DAI and 0.10 for severe DAI, and built tolerance curves for humans as a function of peak rotational velocity and rotational acceleration. Later, Bain et al. [33] performed *in vivo* tests on the optical nerves of guinea pigs and recorded both morphological and functional injury. In this work, strain in the white matter tissue was found to be significantly related to axonal injury. They set an optimal strain threshold value of 0.21 for a 25% probability of morphological injury, and 0.18 for functional injury. Bandak et al. [34] developed a strain-based approach to quantify DAI using a human head FE model. It was called the Cumulative Strain Damage Measure (CSDM) and it is based on the relation of DAI to the total volume fraction of the brain that has overpassed a certain amount of strain at a given time period. The proposed strain threshold value is 0.05 for failed elements. This criterion was applied by Takhounts et al. [24] and posteriorly by Pintar et al. [35], who set the strain threshold at 0.15 as proposed by [24]. Moreover, Pintar et al. suggested the suitability of CSDM as a measure of DAI applied to ballistic loading of a helmeted head.

Focal injury in the brain arises as a consequence of intracranial pressure waves that cause pressure gradients within the skull. Ward et al. [25] found a strong positive correlation between coup intracranial pressures and brain trauma severity and developed the brain pressure tolerance (BPT) curves in terms of acceleration and pulse duration. These curves were built for severe and moderate injury, setting coup pressure limit values of 234 and 172.4 kPa, respectively. They contrasted the BPT with previous existing criteria like the HIC, and found that for short duration impacts (from 0 to 3 ms) the previously developed tolerance curves were not conservative enough. Contusions can also be produced when sustaining high negative pressure values, sufficient to cause cavitation phenomena [30,36]. Gross et al. [37] presented the first study demonstrating the formation of cavitation bubbles in a fluid-filled ellipsoidal glass vessel subjected to impact. Subsequently, Lubock et al. [38] aimed to determine if this phenomenon was likely to take place in living tissues. They performed impact tests upon water-filled human skulls and observed cavitation bubbles at the contrecoup site. However, when replacing the water content by gelatin acting as a brain tissue simulant, there was no cavitation evidence. From these results they stated the unlikeliness of cavitation occurring in the human brain itself but do not deny the possibility of this phenomenon occurring in the CSF and blood vessels which indeed would involve brain damage, even though clinical evidence [39,40] does not yet exist. Takhounts et al. [24] proposed the Dilatation Damage Measure (DDM), a new injury metric, to account for these negative pressure phenomena in the brain. This measure considers the volume of the brain that has experienced pressure values under the water cavitation threshold and is taken as a correlation with contusions suffered in the brain. Nusholtz et al. [41] correlated the acceleration values resulting from a water-filled cylinder struck by an impactor with the risk of collapse resulting from cavitation. They established a 350 g acceleration value as likely to cause violent cavity collapses. In their recent studies, Panzer et al. [39] deepened in the mechanism of CSF cavitation and concluded that the major effect of this process was the increase in brain strains caused by its decoupling from the skull.

As a result of this review, we conclude that experimental testing on BHBT, despite being the preferred method for obtaining real data, presents certain limitations due to the use of PMHS, surrogates and the difficulty to place data acquisition systems on them without altering the results. A possibility to overcome these drawbacks is the use of FE models, although they need to be properly validated to provide reliable results. The prediction of BHBT by means of numerical modelling requires the existence of certain correlations between the measurable mechanical parameters and the different lesions produced in the head tissues. These correlations, the so-called head injury criteria, have been extensively studied under low to medium velocity impact environments, but there are still not specific measures for BHBT. A robust methodology to accurately quantify and predict BHBT injuries is still to be developed.

In this context, the present work aims to analyse the biomechanical effects of ballistic impact on a human head model protected with a combat helmet. The objective is to study non-penetrating impacts under standard test requirements (such as the NIJ standard [15]) so as to relate it to the corresponding biomechanical head injury risks.

The paper is organized as follows. A methodology section that describes the procedures followed. Then, the third section presents the helmet and head modelling and the coupling between both models. It is followed by the results section which is split in three subsections, one for each of the sets of simulations performed. Head injury and other metrics like BFD are computed in this section and later commented in the discussion part, adding the limitations of

2. METHODOLOGY

A finite element model of a human head protected with a combat helmet is obtained in this work to perform ballistic impact simulations using 9 mm FMJ bullets as ammunition. The employed head model was developed in a previous work by the authors [42] and validated against experimental test data from literature on skull stiffness, skull fracture, and intracranial pressures. Additionally, in the present work, this head model has been validated against ballistic impact experiments on PMHS protected heads conducted by Sarron et al. [6]. The aramid helmet shell model was developed and validated against experimental ballistic tests on BFD and V_{50} in [43]. The interior foam padding of the helmet has been modelled in this work following the geometric requirements stated in the Spanish standard for combat helmets [44]. This standard defines two helmet sizes depending on the soldier's head circumference (M and L) which only differ in the thickness of the foam pads. One of the objectives of this paper is to analyse the variation of head injury parameters when the head is protected with an M or an L helmet. Therefore, following [44], the dimensions of the composite helmet shell are maintained for both sizes and we modelled the cushioning with the thicknesses stated for both sizes. The coupling of the helmet shell, padding system and head model is performed by means of Abaqus/Explicit [45] and a modelled 9 mm FMJ bullet is integrated to the assembly.

Departing from this helmeted head configuration, three sets of ballistic FE simulations are performed:

The first consists of a recreation of the NIJ-STD-0106.01 standard for combat helmets against 9 mm FMJ ammunition, replacing the dummy/clay headform used in impact testing by the image-based human head model. The boundary conditions applied to this set of simulations correspond to the experimental parameters established in the aforementioned standard, which consists of four shots with a bullet velocity of 358 ± 15 m/s, each of them taking place at a different location: frontal, temporo-parietal (right side), occipital and vertex. All the simulations corresponding to this set are performed with the M size helmet configuration. Posteriorly, the head injury criteria presented in Table 1 are computed and discussed for each of the performed impacts.

The two remaining sets of simulations aim to analyse the influence of other parameters (the impact velocity and foam padding thickness), which seem to be determinant for closed head injury occurrence and its transition to open head injury (when the skull fractures).

In this line, a second set of simulations is performed varying bullet initial velocity in the range from 425 up to 615 m/s, depending on impact location. The upper velocity limit corresponds to the maximum 9 mm bullet speed that the helmet can withstand without penetration. Again, the M size helmet is employed in this analysis. Skull internal energy and cranial fracture patterns are recorded for each velocity studied.

Finally, the third set of simulations assesses the effect of head size and padding thickness on head injury. The baseline 55 cm-circumference head model is replaced by a 61 cm one and, following the conditions stablished in [44], an L size helmet is employed. Under this setup, shot simulations are performed first under the conditions stated by NIJ-STD-0106.01 and then varying

the initial bullet velocity. Again the head injury criteria from Table 1 are computed and compared to the values obtained in the first set of simulations to capture the differences between both helmet sizes. Additionally, the results from the parametric analysis in terms of bullet velocity are contrasted with the ones from the second set.

3. FE MODELLING

3.1. Head model

The head numerical model employed for the ballistic simulations is the one developed in Lozano-Minguez et al. [42] based on computed tomography (CT) images of an anonymous middle-aged male subject. The level of detail achieved in the model is similar to that used in other established head models, considering six differentiated layers: scalp, compact bone, diploë, face bone, cerebrospinal fluid (CSF) and brain.
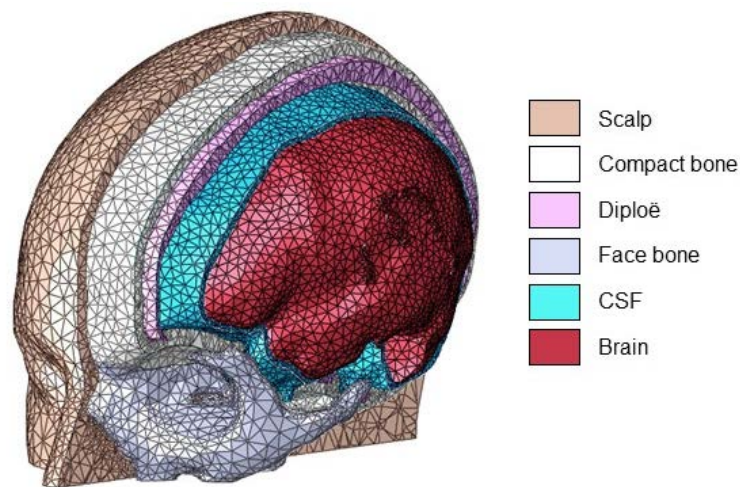

Fig. 1. Human head FE model developed from CT images.

Scalp, skull bones, and CSF were considered to behave as linear-elastic materials in our model as in the majority of human head models from the literature [26,46–50]. The brain is surrounded by the meninges, which consist of three layers of protective tissue: dura mater, arachnoid mater, and pia mater. The subarachnoid space, located between the arachnoid mater and the pia mater, is filled with the CSF and contains fibrous filaments in order to prevent excessive movement of the brain. Therefore, the CSF layer is modelled using linear elastic solid elements with low shear modulus to structurally represent this set of tissues and to allow relative motion of the brain [24,51].

In order to deal with scalp and skull fracture a failure model is implemented to allow element erosion at the fracture zone. The maximum normal stress criterion (Rankine's criterion) is implemented and the elements are eliminated by a VUSDFLD subroutine [52]. The ultimate strain threshold value for scalp is set at 70% [53], and ultimate compressive and tensile stress threshold values are 24.8 and 34.8 MPa for diploë, and 132 and 90 MPa for compact bone [23], respectively.

A Mooney-Rivlin hyperelastic constitutive law [54,55] is used for representing the brain behaviour. Additionally, rate effects are taken into account through linear viscoelasticity defined by a Prony series expansion of the dimensionless relaxation modulus [45]. A summary of the mechanical properties considered in this study is provided in Table 2.

	Scalp	Diploë	Compact bone	Face bones	CSF	Brain		
Density (kg m⁻³)	1130	1500	1800	3000	1000	1040		
Young's Modulus (MPa)	16.7	4500	15000	5000	1.26[a]	**Hyperelastic constants[b]**	C_{10}=62 Pa, C_{01}=69 Pa	
Poisson's ratio	0.42	0.22	0.21	0.21	0.4999	**Viscoelastic constants[c]**	g_1=0.636 g_2=0.363	τ_1= 0.008 s τ_2=0.15 s

[a] Equivalent *E* for a solid with fluid properties.

[b] Constants for the implementation of a Mooney-Rivlin material in *Abaqus* [54,55].

[c] Shear relaxation terms for a Prony series in *Abaqus* [45].

This human head model was validated against the experimental data provided by Yoganandan et al. [56] and Nahum et al. [57] in their low-velocity impact tests on PMHS. Some of the results of this validation are illustrated in Fig. 2 showing the accuracy of the model when predicting experimental reaction force and ICP in [56,57] with results close to the experimental curves from these experiments. Further details of the validation procedure can be found in [42]. Additionally, the head model has been also validated against the ballistic experiments from Sarron et al. [6] on post-mortem human heads using 9 mm FMJ bullets and different protective materials. Specifically, the tests simulated correspond to nº27, 68 and 72 from [6]. In the first one, the protective material consists of a 250 mm-diameter aluminum plate located with no offset distance with respect to the parietal region of the head. In the remaining two cases, the plate is made up from aramid and the offset distances are 0 mm (nº68) and 8 mm (nº72). Our simulations show that tests nº27 and nº72 do not lead to skull fracture, in contrast to test nº68 where a clear comminuted-depressed fracture is predicted. These injury patterns coincide with the ones reported in [6]. Pressure values measured at the cisterna magna of the head (close to the posterior fossa) are recorded, and reveal to be in the same order of magnitude than the experimental values. The main results obtained from this validation are summarised in Table 3.

Table 3
Data for ballistic simulation of the head model against experimental tests by Sarron et al. [6] .

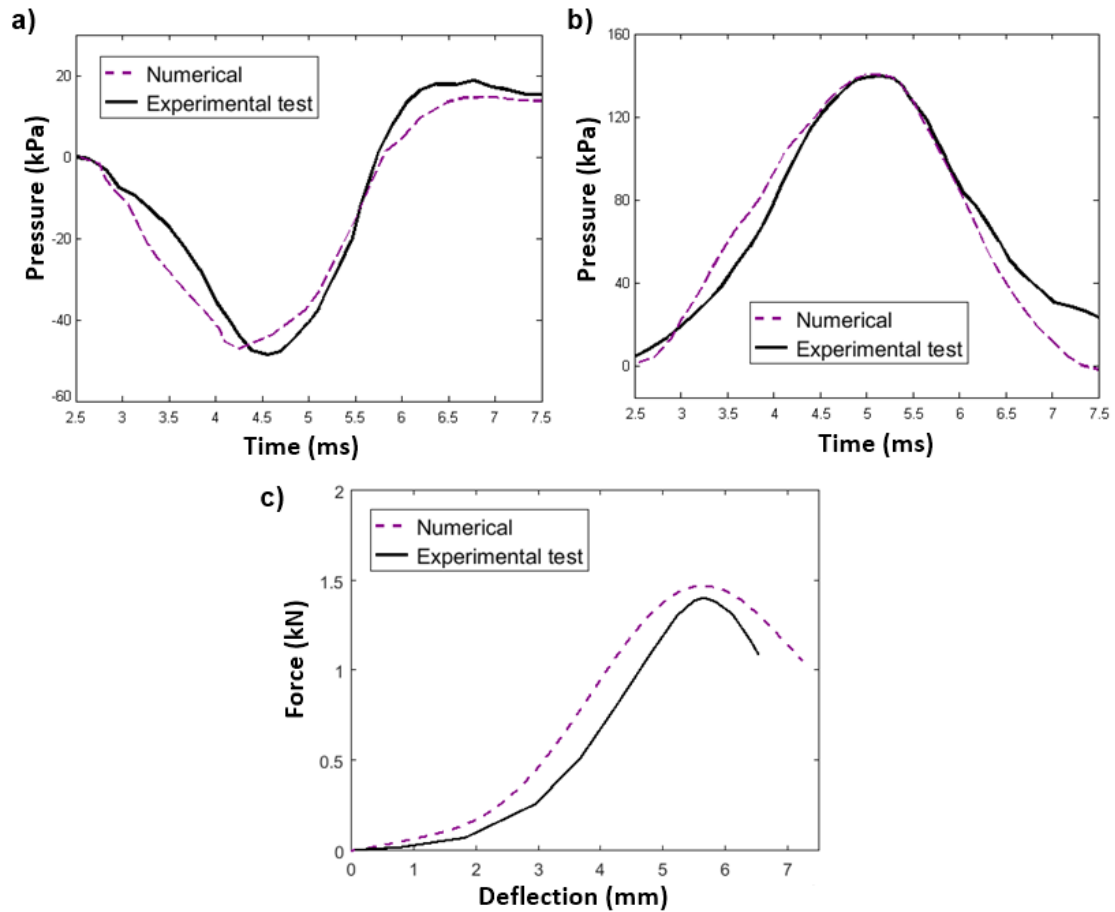| Test ID	Plate-head distance (mm)	Plate material	Bullet velocity (m/s)	Experimental cisternal pressure (kPa)	Simulated cisternal pressure (kPa)
27	0	Aluminum	383	40	52
68	0	Aramid	388	193	180
72	8	Aramid	386	25	26

Fig. 2. Numerical head model validation in terms of predicted and experimental intracranial pressure ICP in a) occipital region and b) frontal (Nahum et al. [57]*) and c) force (Yoganandan et al.* [56]*).*

3.2.   Helmet and ammunition models

A common combat helmet consisting of a hard composite shell and an interior pad system designed under standard NIJ is also modelled. In this work, the shell helmet is made of layers of aramid bonded by a thermoset resin acting as the matrix material. C3D6 elements with element size equal to 4 mm are used to model the shell combat helmet (see Fig. 3). Moreover, four element layers through the helmet shell thickness are considered in order to reduce computational cost and increase computational efficiency. Model validation was carried out in a previous work of the authors dealing with the mechanical design of the helmet [43].

The mechanical properties of combat helmets are taken from Tan et al. [58]. The design of the combat helmet was validated by previous work of the authors through experimental tests using STANAG 2920 and NIJ-STD-0106.01 standards. For more details see reference [43].

The aramid composite is assumed to have elastic behaviour up to failure. Hashin failure criterion for fabrics is implemented by a user subroutine VUMAT in order to predict the failure of the aramid composite. The failure modes are presented in Table 4:

Table 4.
Mechanical behaviour of Kevlar composite [43].

Failure mode	Hashin fabric failure criterion
Tensile Fiber Failure $(\sigma_{11}, \sigma_{22} > 0)$	$d_{1t} = \left(\dfrac{\sigma_{11}}{X_{1T}}\right)^2 + \left(\dfrac{\tau_{12}}{S_{12}}\right)^2 + \left(\dfrac{\tau_{13}}{S_{13}}\right)^2$ $d_{2t} = \left(\dfrac{\sigma_{22}}{X_{2T}}\right)^2 + \left(\dfrac{\tau_{12}}{S_{12}}\right)^2 + \left(\dfrac{\tau_{23}}{S_{23}}\right)^2$
Compressive Fiber Failure $(\sigma_{11}, \sigma_{22} < 0)$	$d_{1c} = \left(\dfrac{\sigma_{11}}{X_{1C}}\right)^2 + \left(\dfrac{\tau_{12}}{S_{12}}\right)^2 + \left(\dfrac{\tau_{13}}{S_{13}}\right)^2$ $d_{2c} = \left(\dfrac{\sigma_{22}}{X_{2C}}\right)^2 + \left(\dfrac{\tau_{12}}{S_{12}}\right)^2 + \left(\dfrac{\tau_{23}}{S_{23}}\right)^2$
Tensile Inter-ply Matrix Failure (delamination) $(\sigma_{33} > 0)$	$d_{mt} = \left(\dfrac{\sigma_{33}}{X_{3T}}\right)^2 + \left(\dfrac{\tau_{13}}{S_{13}}\right)^2 + \left(\dfrac{\tau_{23}}{S_{23}}\right)^2$
Compressive Inter-ply Matrix Failure $(\sigma_{33} < 0)$	$d_{mt} = \left(\dfrac{\sigma_{33}}{X_{3C}}\right)^2 + \left(\dfrac{\tau_{13}}{S_{13}}\right)^2 + \left(\dfrac{\tau_{23}}{S_{23}}\right)^2$

The parameters in Table 4 are the following: σ_{11}, σ_{22}, and σ_{33}, are the stresses in longitudinal, transverse and through-thickness direction respectively; σ_{12}, σ_{23}, and σ_{13}, are the shear stresses; X_{1T} and X_{2T} are the tensile strengths in the warp and weft directions; S_{12}, S_{13}, and S_{23}, are the transverse shear strengths. Failure occurs when any damage variable (d_{ij}) reaches the value of one.

The foam padding is meshed with 6008 hexahedron elements (type C3D8R in Abaqus, see Fig. 3). Their mechanical behaviour is modelled using the Low Density Foam material model available in Abaqus which is intended for low-density, highly compressible elastomeric foams with significant rate sensitive behaviour, such as polyurethane foam.

According to NIJ-STD-0106.01 [15], which establishes the performance requirements and methods of testing helmets intended to protect the wearer against small calibre guns, the ammunition considered in this work is 9 mm Full-Metal Jacketed (FMJ) bullet weighing 8 g (124 grain). The FMJ bullet consists of the lead core and the copper jacket. The lead core is modelled with five hundred and sixty elements and its mechanical behaviour is assumed to be elastic-plastic characterised by an equation of state (EOS). One hundred and ninety elements are used in discretizing the copper jacket and its mechanical behaviour is carried out using Johnson Cook model and damage initiation criterion (see Fig. 3). More details of helmet modelling can be obtained in a previous work of the authors [43].
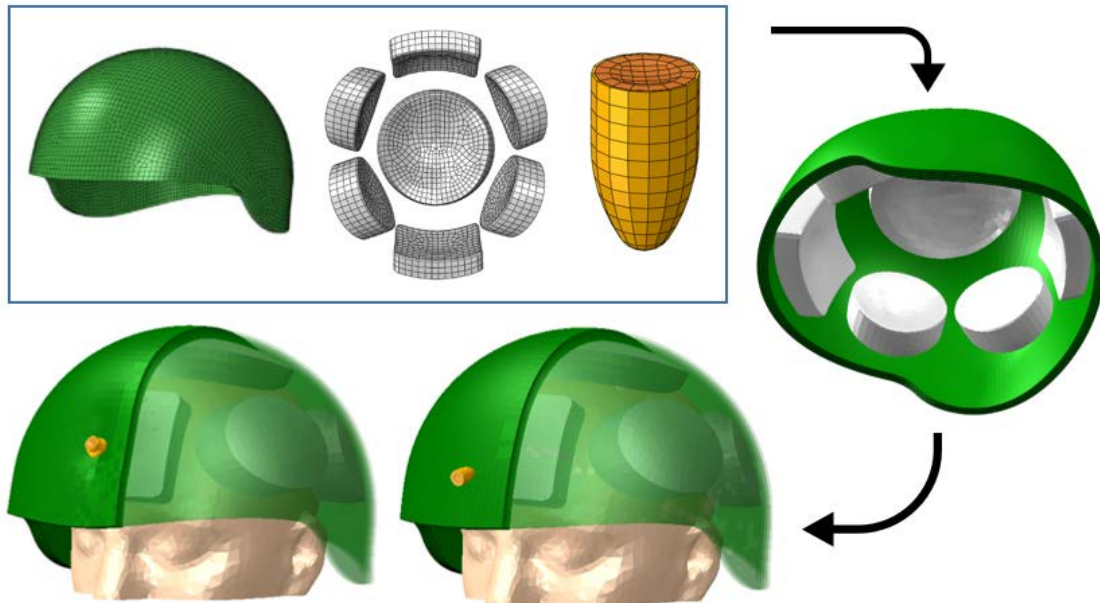
Fig. 3. Top: helmet shell, foam padding and bullet meshes. Bottom: head-helmet coupling with Abaqus/Explicit for ballistic simulations.

3.3. Interaction and Boundary Conditions

The coupling between the helmet and the head model is carried out by means of an Abaqus/Explicit [45] low-velocity simulation in order to ensure a proper adjustment between the helmet padding and the head representing the current wearing of the helmet. The final head-foam-helmet configuration is illustrated in Fig. 3 (bottom).

The general contact algorithm available in Abaqus/Explicit with a hard contact interaction property [45] is used to model the interaction between the helmet and the head, and between the bullet and helmet. Specific surface-to-surface contact properties are set between the helmet composite layers and the union between the bullet core and its jacket. Artificial strain energy is recorded in all the analyses and maintained at a value less than the 1% of the internal energy, to ensure that no hourglass problems arise [45].

Initial velocity boundary conditions are set to the bullet model, changing their value and direction according to each of the analysis stated in Section 2.

4. RESULTS

4.1. Simulation of helmet testing standard NIJ-STD-0106.01

As it was explained previously, the shots impacting at different head zones (frontal, temporo-parietal right side, occipital and vertex) are simulated reproducing the tests defined in NIJ-STD-0106.01. Transient BFD configurations for each shot corresponding to a time of 0.2 ms are illustrated in Fig. 4. In all of the cases the simplified helmet model accomplishes the accepted thresholds of BFD stated by the normative, and none of them reveals fibre breaking at the inner layer.

Seven of the head injury criteria, summarised in Table 1, have been selected and calculated from our numerical results for the assessment of both skull fracture and brain injury. The first set are acceleration-based criteria, and some of them (HIC_{15}) are still being used in helmet design. However, it remains unclear whether they are able to predict skull fracture over any impact condition. For this reason, they will be compared to the criterion of cranial ultimate stress and their applicability to the high-velocity environment will be discussed. Concerning brain injury, the strain-based approach of CSDM is taken to measure the likeliness of diffuse injuries, whereas for focal injuries (contusions) the DDM and maximum ICP criteria are chosen.

Despite being a short-duration event whose effects are fully attenuated after 5 ms, the simulations are performed for a 15 ms period in order to evaluate the HIC_{15} parameter, as it was previously explained. Derived from the HIC_{15}, the SFC and Hertz's [22] fracture probability are computed. For the assessment of brain trauma, cumulative values of DDM and CSDM are calculated from the pressure and strain time history, respectively. Additionally, maximum intracranial pressures (ICP) are recorded. All these results are gathered in Table 5.
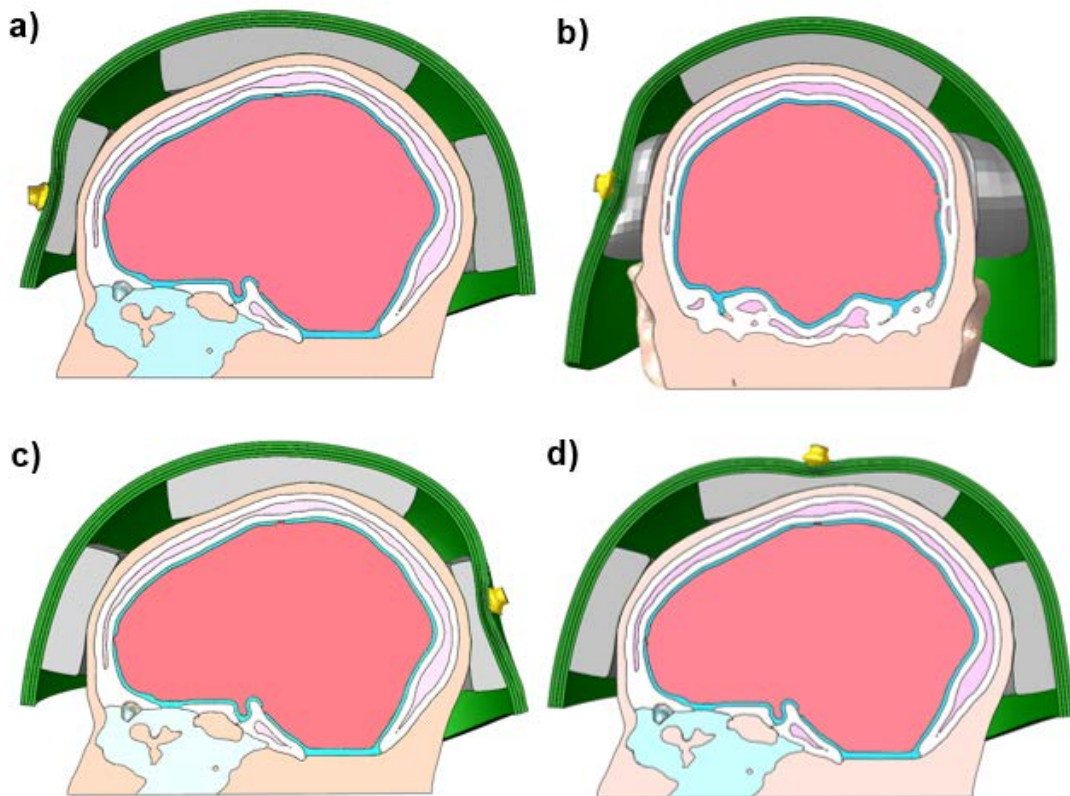

Fig. 4. Abaqus/Explicit simulations of the NIJ standard for helmet testing at the different head regions: a) frontal, b) temporo-parietal, c) occipital, d) vertex.

	Frontal	Lateral	Occipital	Vertex	Critical Values
HIC$_{15}$	262.18	345	285	533	700 [20]
SFC (g)	50.4	56.2	52.1	66.9	120 [21]
P(fract)	5%	9.4%	6.1%	20%	measured as probability [22]
DDM	89%	96%	97%	99%	7.2% [24]
CSDM	0%	0%	0%	0%	55% [24]
Peak ICP (kPa)	243	250	260	460	234 [25]

4.2. Effect of impact velocity on head injury

There is a wide range of impact velocities that the helmet can withstand without being perforated by the bullet. As the initial kinetic energy of the projectile increases, the helmet experiences more severe damage due to delamination and fibre breakage. This structural damage begins at the inner composite layer (the one in contact with the cushioning) caused by bending stresses and makes the helmet shell more compliant at the impact site, therefore the backface deformation increases. This rise will be proportional to the magnitude of the blow delivered to the head, since both the strain rate at the BFD region and the contact area, are increased. Taking the frontal and right-lateral shot cases, bullet initial velocities are varied from 425 m/s up to the value necessary to produce the perforation of the helmet. Skull fracture probability and brain trauma are analysed.

Skull peak internal energy (IE) appears to be the most suitable fracture predictor for both frontal and lateral cases, in agreement with the findings of Sahoo et al. [23]. The internal energy calculated for the case of frontal shot simulations is shown in Fig. 5. The sudden increase of the peak internal energy as a function of velocity coincides with the limit for intact skulls and the transition to fractured skull cases (590-600 m/s). The first case leading to skull fracture, corresponding to a bullet velocity of 595 m/s presents the linear fracture pattern shown in Fig. 6 top, similar to that reported by Delye et al. [59]. Crack initiation is reached for a skull internal energy value of 4 J. Greater velocities result in multiple cracks and comminuted-depressed fractures at the impact site (Fig. 6 bottom). Deformation and damage patterns on the helmet impacted region for each shot are represented in Fig. 5, showing a link between composite layer breakage and skull internal energy. The transition between the injured and non-injured cases is determined by the damage suffered in the third layer of the simplified helmet model. When two of the four layers remain unbroken (being equivalent to half of the thickness being undamaged), the helmet retains its protective effect against skull fracture. In terms of BFD values, a 26-27 mm displacement of the composite shell is sufficient to cause severe injury in the head, while greater magnitudes would not be reachable because the complete penetration of the bullet would occur.
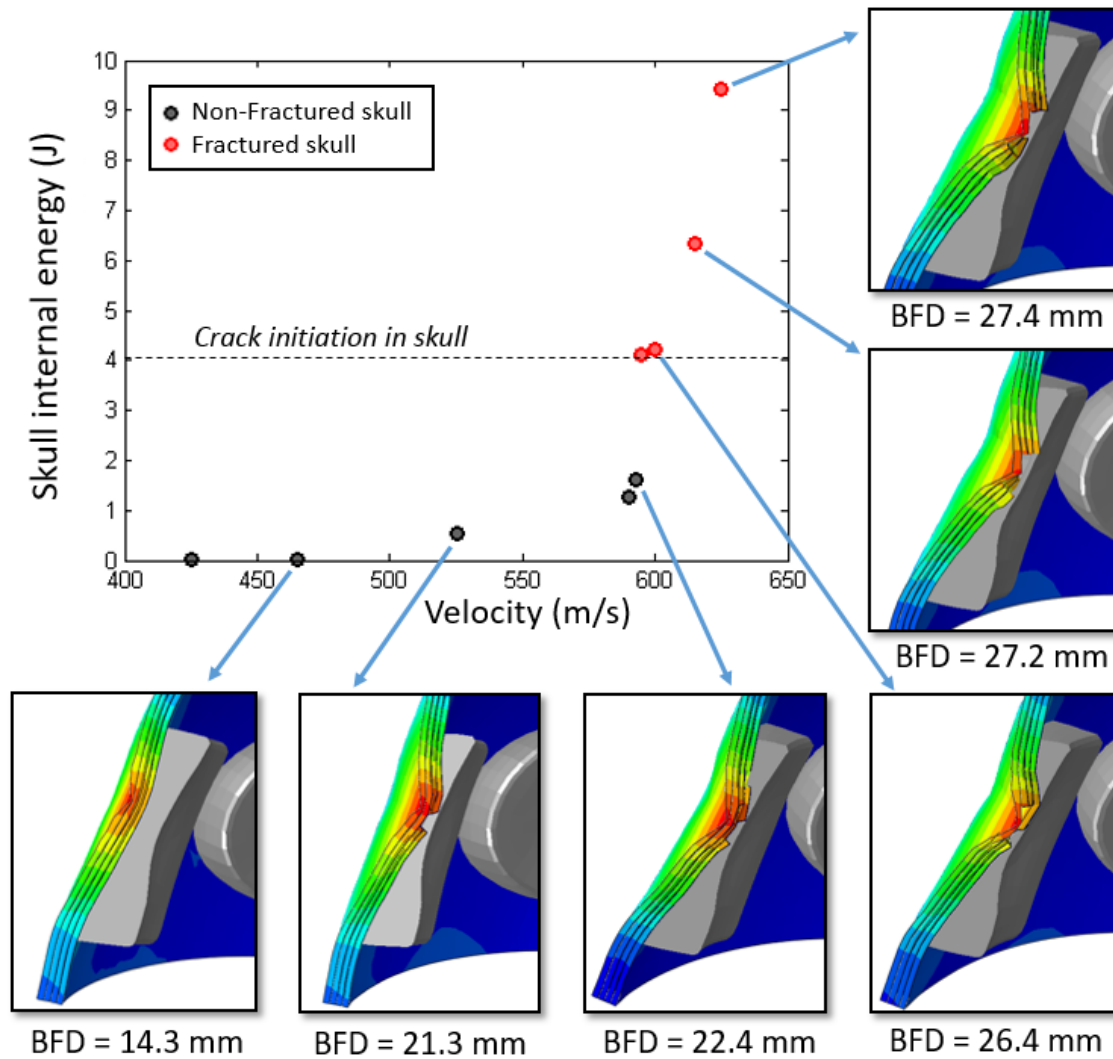
Fig. 5. Peak skull internal energy for different impact velocities at the frontal site using an M-size helmet. Corresponding backface deformation patterns for each velocity case.

The breakage of the cranial vault is likely to enhance other mechanisms of injury in the brain tissue, although severe brain injuries are not necessarily linked to the presence of skull fractures [60,61]. In the comminuted-depressed fracture cases simulated, CSDM levels rise with respect to the non-fractured cases from 0 to 8% due to a greater deformation in the brain at the impact site caused by the loss of the protective cranial shell integrity.
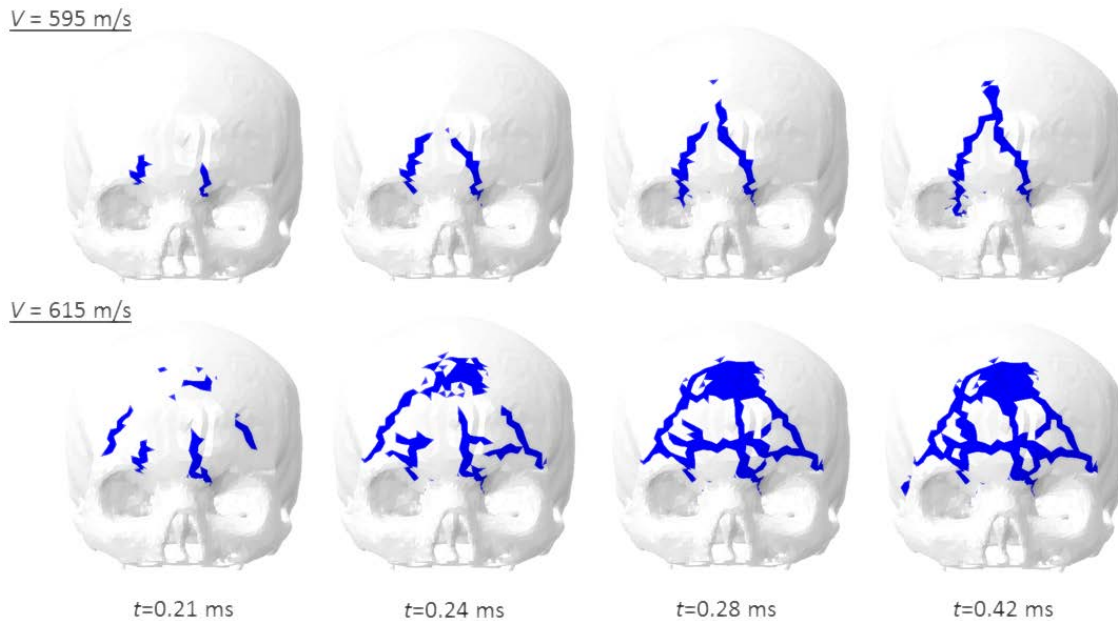
V = 595 m/s

V = 615 m/s

t=0.21 ms   t=0.24 ms   t=0.28 ms   t=0.42 ms

Fig. 6. Skull fracture temporal evolution for bullet velocities of 595 and 615 m/s in the ballistic simulations using an M-size helmet.

Fig. 7 presents the peak internal energies obtained at different bullet velocities for the lateral impact. Internal cracks as the one depicted in the top of Fig. 8 initiate when the internal energy reaches a value of 1.63 J, lower than the required for frontal bone fracture. This more brittle behaviour is probably due to the reduced thickness of the diplöe layer at the lateral impact site. Regarding helmet shell deformations, the trend observed in the frontal shooting cases is followed and the first cranial cracks appear when the three inner layers break. However, the BFD value at which skull fractures is achieved is 24.2 mm, lower than its corresponding value for frontal impact.

Thus, results for lateral impacts reveal lower resistance of cranial bone in the temporo-parietal region. This finding is in agreement with Zhang et al. [49] that reports greater strains in the lateral skull region rather than in the frontal one. A shot of 540 m/s results in cracks in the inner compact bone layer and diplöe at the temporo-parietal region (Fig. 8 top). Fractures along the entire thickness of the cranium are achieved for bullet velocities over 545 m/s presenting depressed fragments of the outer compact bone layer. Additionally, some non-critical surface cracks are observed at the middle-posterior skull base. These patterns are similar to those shown by Sarron et al. [6], although they also observed linear fractures associated with the circular comminuted ones. This difference is due to the use of distinct protective materials to simulate the helmet shell and stand-off distances.
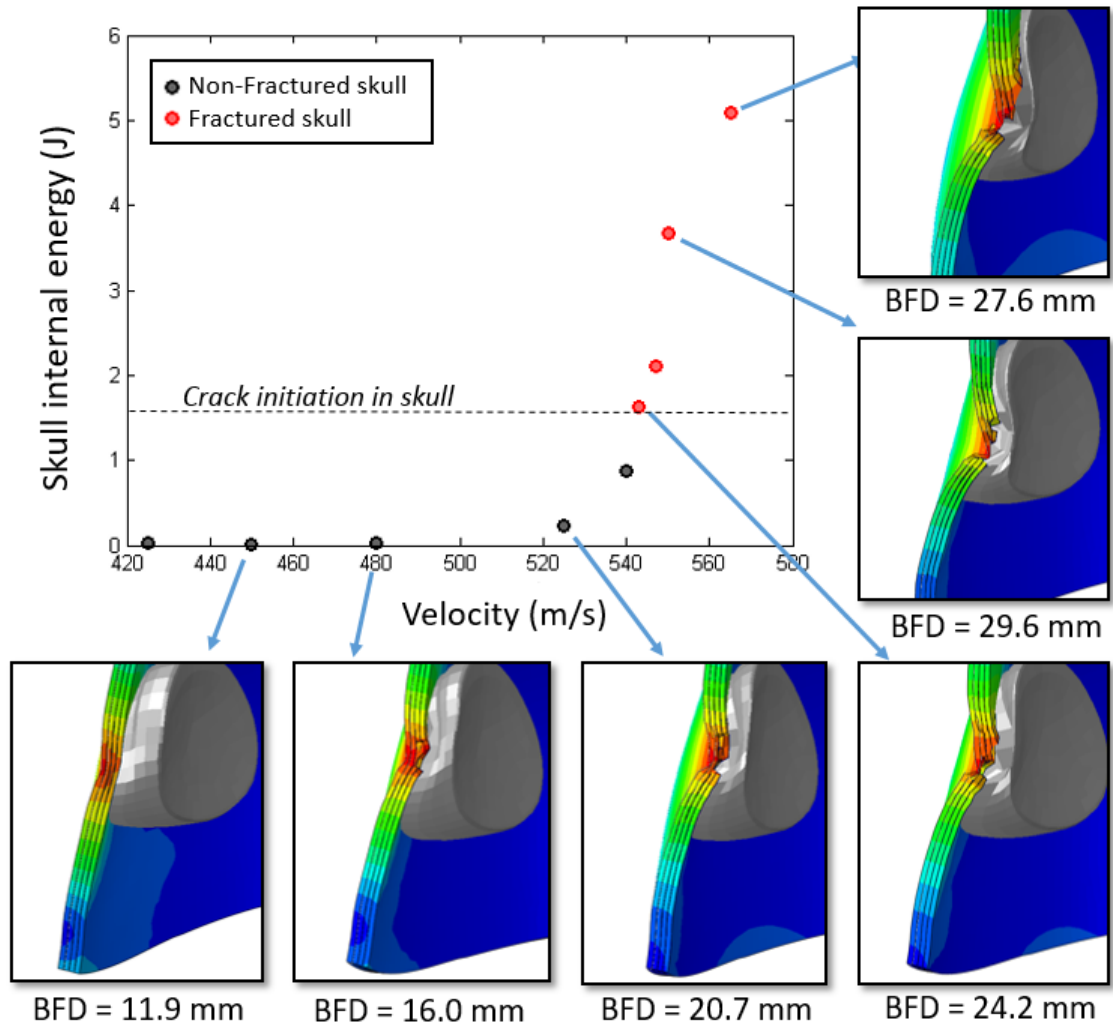
16

Fig. 7. Peak skull internal energy versus bullet initial velocity in lateral ballistic simulations with an M-size helmet. Maximum right side backface deformations for each velocity case.
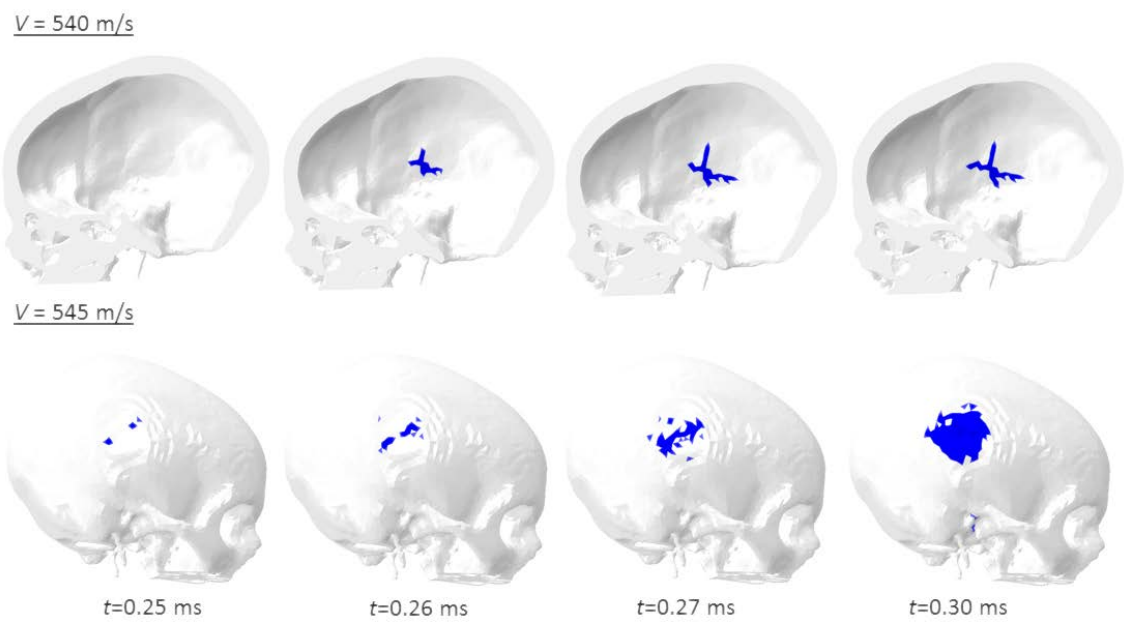

Fig. 8. Temporo-parietal crack evolution for lateral shots with the baseline M-size configuration at 540 and 545 m/s showing internal and external fractures, respectively.

4.3.　　　Effect of head dimensions and padding thickness

As mentioned in Section 2.3, the head model developed for the previous analyses has a circumference of 55 cm. Helmet manufacturers do not provide tailored-made protections that adjust the exact size of the head. Usually, there exist a few available sizes for each helmet model although it depends on the standard they are subjected to, and the countries where it is accepted. For instance, the Spanish standard [44] adapts the NIJ requirements and states two helmet sizes (M and L). In this case, the shell size is the same, while the foam padding system presents two possible thicknesses depending on the soldier head dimensions. For head circumference values greater than 59 cm, the cushioning must be reduced from 1.9 cm (size M) to 1.3 cm (size L). This fact is likely to affect the overall performance of this protective system as both the stand-off distance and the energy absorbed by the padding will change. The results presented in this section will be based on these specific requirements as an example of the existing helmet sizing methodologies. The head model was scaled to 61 cm-circumference to study the previously mentioned phenomena.

The reduction in padding thickness leads in general to a higher injury risk. Repeating the frontal shot simulation from the NIJ testing protocol with the large head model yields the results shown in Table 6. All injury indicators yield higher values than the M-size case, especially in the parameter P(fract) developed by Hertz [22].

Table 6.
Injury metrics for the L-size helmet configuration at the frontal site.

	Frontal impact on M-size helmet	Frontal impact on L-size helmet
HIC$_{15}$	262.18	659.5
SFC (g)	50.4	72.8
P(fract)	5%	28.9%
DDM	89%	95%
CSDM	0%	0%
Peak ICP (kPa)	243	340
Critical bullet velocity for skull fracture (m/s)	595	523

Another set of simulations varying the initial bullet velocity is performed and the results are in agreement with the statement that lower stand-off distances due to decreased foam pad thickness result in increased damage [6,13].

Plotting skull internal energy versus velocity (Fig. 9) reveals that a lower velocity threshold is necessary for the prediction of skull fracture in comparison with the head baseline numerical model used in Section 3.2. The minimum BFD value causing fracture is 18.2 mm, and only the inner layer of the simplified shell model is broken at this stage.
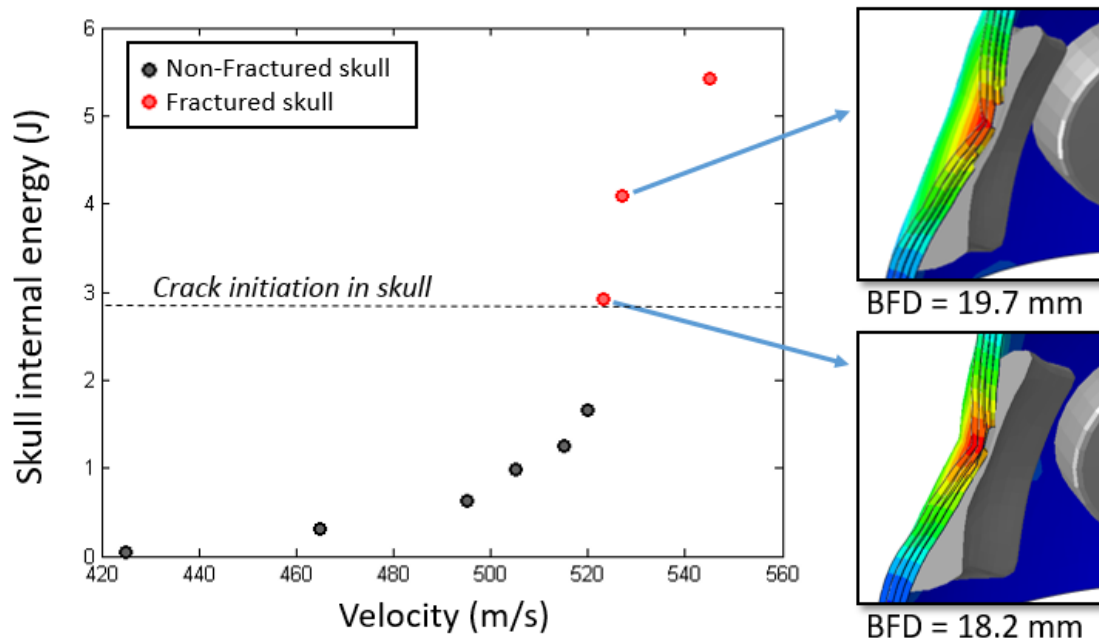
Fig. 9. Peak skull internal energy versus bullet initial velocity with the L-size helmet. Fracture initiation threshold in cranial tissue at 2.8 J.

Fig. 10 shows skull fracture patterns evolution: fracture conditions are achieved at a much lower bullet velocity (523 m/s) than the required for the M-size helmet. It is observed from the results obtained that the cracks initiated at the forehead tend to propagate towards the base of the skull. A basilar skull fracture (BSF), which is any fracture that begins at or propagates through the base of the skull, causes brain stem injuries and haemorrhages that can provoke instantaneous death [62]. Specifically, a frontobasal fracture, like the one obtained in the analyses and depicted in Fig. 10 (top), is likely to produce coma and sensorial deficiencies [63].
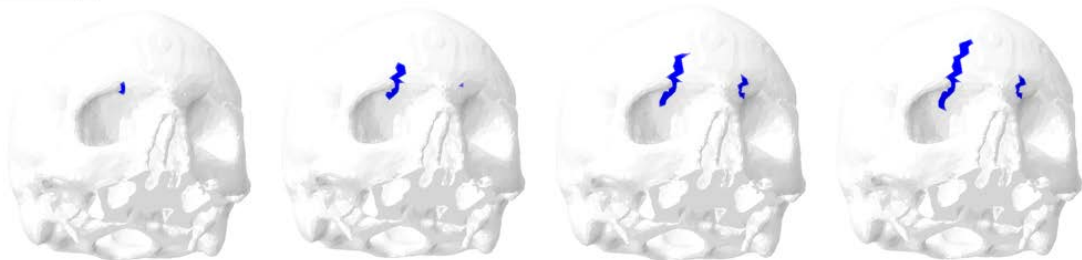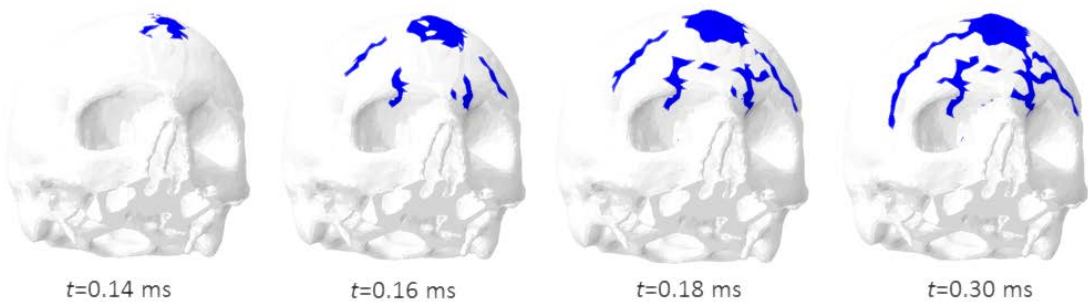

Fig. 10. Time evolution of skull fracture in L-size helmet simulations for bullet velocities of 523 and 530 m/s in a frontal shot.

5. DISCUSSION

Although BFD is one of the most used measure in combat helmet testing standards, there is no direct link between this parameter and the actual head tissues response. In order to address this important biomechanical issue giving the real level of protection of the current standard limits, some injury mechanisms regarding skull fracture and brain damage are studied through the FE simulations.

Section 4.1 presents the results from recreating the NIJ standard conditions using human head model. Results summarized in Table 5 reveal that the tested helmet offers an adequate protection in terms of head accelerations, since none of the cases yields critical values of HIC and its derivatives. This result is in line with the experimental tests conducted by Freitas et al. [7]. The same trend is observed in terms of brain strain, as the CSDM remains null even though using the most conservative value for the threshold deformation (5%). The FE head model does not include any method for cavitation prediction in CSF so its effect upon brain tissue strain [39] cannot be captured. However, the strain field obtained within the brain model for all the cases of study has peak values in the order of 10-3. This means that even accounting for the presumable strain amplification caused by CSF collapse, no significant change in CSDM values would be observed. Therefore, the current combat helmet provides proper prevention from axonal dysfunction under the ballistic conditions stated by the normative.

Nonetheless, ICP values exceed the safety thresholds that have been most widely accepted in literature concerning both positive and negative limits. Resulting DDM values suggest that, for all the simulations considered, almost the entire brain volume withstands pressures below the water cavitation limit, which would involve more than 95% probability of brain contusion according to Takhounts et al. [24]. The link between cavitation and brain injury is not fully understood yet, but there is a risk of damaging the brain blood vessels that should not be ignored. Regarding peak ICP, the frontal shot presents the lowest value but it is still over the 234 kPa threshold for severe brain injury proposed by Ward et al [25]. ICP values obtained are in the same range than the ones reported experimentally by Sarron et al. [6] for lateral impacts and by Freitas et al. [7] for frontal shots, both using the same ammunition. Experimental shots conducted by Rafaels et al. [8] on PMHS at similar velocities resulted in dural contusion and separation of the dura from the skull. Although the authors did not directly associate these injuries as aftermath of the impact, this possibility is not discarded. Therefore, it remains unclear whether the simplified combat helmet is efficient in the mitigation of focal brain injuries such as contusions.

Therefore, results presented in Section 4.1 highlight the need of consideration of the injury mechanisms resulting from ICP and their insertion into the current combat helmet testing methodologies. Furthermore, translational acceleration-based parameters do not show an evident biomechanical link with the real response in brain tissue, so they should not be taken as the unique measure in the assessment of head injury, especially for ballistic impact.

A further understanding of the helmet behaviour under higher velocity impacts is achieved through the parametric study presented in Section 4.2. The damage level suffered by the helmet after the bullet impact directly affects the energy transmitted to the skull and thus the injury risk. Skull internal energy is taken as the optimal measure for skull fracture prediction, agreeing with Sahoo et al. [23]. However, the energy values leading to cranial fractures in the simulations performed (depicted in Figures 5 and 7 for frontal and lateral impacts, respectively) are one

order of magnitude greater than the threshold of 453 mJ proposed in [23], which is not based in ballistic impact. This discrepancy can be related to the different nature of ballistic impact and accidental falls. Yoganandan et al. [56] and Delye et al. [59] suggested that the mean energy absorbed by the skull until fracture under dynamic loading conditions is 23.51 and 22-24 J, respectively, showing no significant dependency on impact velocity. Nonetheless, it was not proved in their studies that an unrestrained skull would behave in the same manner as in their experimental tests. In addition, no previous internal energy threshold has been developed in literature to assess skull fracture in a helmeted head on the ballistic applications. In this work, we have estimated the skull fracture as a function of the impact velocity using our numerical model. Fig. 6 demonstrates that increasing the initial kinetic energy of the bullet results in a more severe fracture pattern that triggers other brain injury mechanisms (DAI).

The effect of reducing the stand-off distance as a result of keeping constant the helmet shell dimensions is presented in Section 4.3. Results reveal that a 30% reduction of the padding thickness diminishes the critical bullet velocity for causing skull fracture by a 13%. As observed in Fig. 10, the likeliness of the cracks to propagate along the base of the skull leading to more severe injuries is also increased with the reduced stand-off. Furthermore, the recorded BFD values are lower for the L-size helmet simulations for each of the velocities tested. The critical value for this deformation measure falls to 18.2 mm with respect to the 26 mm obtained with the baseline model. According to the helmet standard, BFD values lower than 20 mm are acceptable, but the results obtained in this work reveal that this threshold does not prevent from head injuries like skull fracture when the head size is increased. Therefore, this study suggests that for an adequate injury risk evaluation in combat helmet testing, it is necessary to perform specific impact velocity-risk curves for each of the PMHS heads tested. Otherwise, the usual dispersion between the metrics of the specimens tested may lead to varied conclusions. Additionally, we remark that, for an adequate level of protection, the helmet composite shell should be properly sized in order to maintain the same stand-off distance for all the available sizes. Other possibility is, if the shell dimensions are kept the same in order to facilitate the manufacturing process, to incorporate helmet inserts like the one presented by Ning et al. [64].

The conclusions achieved in this work provide certain biomechanical basis to improve the protection level of current composite combat helmets. However, the study presents some limitations:

• The validation procedure for the head model is based on experimental tests on PMHS. Therefore, it is uncertain whether the in vivo behaviour of the different tissues is fully captured with the applied material laws.

• The human head model is not fully detailed and some missing structures like the falx cerebri and the tentorium may affect the impact response of the brain. These and other relevant intracranial structures will be included in further works.

• The helmet shell is modelled in four layers to save computational cost. Modelling all the real composite layers would give a more detailed insight of the helmet response to bullet impact. Effects as ply breakage and delamination could be more deeply studied.

• The strapping system of the helmet has not been modelled. Although its effect would be negligible at the first stages of the impact, it would be important to include it for longer simulations, as it would affect the head kinematics. The same reasoning would apply for the absence of a neck model.

6. CONCLUSIONS

This work provides biomechanical considerations that should be taken into account when designing combat helmets and, specifically, their padding system. Although the objective of standards is always guaranteeing a minimum protection level of personal protections, testing and requirements stated in standards focus on mechanical parameters of the impact process, defining projectile type, impact velocity and BFD of the helmet. No biomechanical issues are addressed due to the difficulty due to the difficulty to develop experimental analyses. In this work the study of the consequences of non-penetrating high-speed ballistic impacts upon a human head wearing a combat helmet by means of FE modelling is presented. The effectiveness of current helmet testing standards in the prevention of head injury is discussed in terms of damage indicators established in the literature.

Some conclusions can be drawn from this work:

- BFD, which is one of the most common measures for combat helmet acceptance (from a safety point of view) cannot be solely responsible of guaranteeing the protection against brain trauma as ICP peak values exceed the injury thresholds even when BFD values remain below their tolerance limits.
- Current acceleration-based criteria like HIC_{15} fail to predict properly some injury mechanisms arising from short-duration impact events, like focal injuries (contusions) as the ballistic accelerations are known to be far below any injurious level.
- As a result of our numerical investigation, we can conclude that the skull internal energy can be a good predictor for skull fracture, in agreement with the findings of Sahoo et al. [23]. The skull internal energy as measured from a FE analysis provides useful information when plotted versus the bullet velocity. This plot is highly nonlinear and the steep increase in skull internal energy indicates the onset of critical bullet velocity. For our head model, and for M-size helmet with a stand-off distance of 19 mm, tolerance for frontal bone is set at 4 J, while for the temporo-parietal bone crack initiation is found at 1.63 J. Critical bullet velocities are found to be 595 m/s for frontal linear fractures and 615 m/s for linear and comminuted-depressed fractures. In lateral shot simulations, the critical bullet velocity is less than for the frontal case. Comminuted-depressed fractures are found for impact velocities beyond 545 m/s.
- Head size and the thickness of the helmet pads become a relevant factor when the helmet shell dimensions are not proportionally adapted to maintain the stand-off distance. In a 61 cm-circumference head, the critical bullet velocity falls to 523 m/s. This scale effect should be taken into account in ballistic that makes use of PMHS by adapting the injury risk curves to the anatomy of each specimen tested.

Despite the complexity of studying biomechanical damage indicators, the methodology presented in this paper, based on finite element analysis, can be implemented in the design process of head protections. On the other hand, standards should include more conservative regulations and try to account for biomechanical considerations, although this is still far from becoming conventional and it is a goal to be achieved in the future. Increasing the understanding of the process would allow to implement simple actions like providing proper shell helmet size, that would significantly improve the protection level of the helmet.

REFERENCES

[1] Folio L, Solomon J, Biassou N, Fischer T, Dworzak J, Raymont V, Sinaii N, Wassermann EM, Grafman J. Semi-automated trajectory analysis of deep ballistic penetrating brain injury. Military Medicine, 178(3): 338–345

[2] Kulkarni SG, Gao X-L, Horner SE, Zheng JQ, David NV. Ballistic helmets – Their design, materials, and performance against traumatic brain injury. Compos Struct 2013;101:313-331.

[3] Hisley DM, Gurganus JC, Drysdale AW. Experimental methodology using digital image correlation to assess ballistic helmet blunt trauma. J Appl Mech 2011;38(5) ASME.

[4] Van Hoof J, Cronin DS, Worswick MJ, Williams KV, Nandlall D. Numerical Head and Composite Helmet Models To Predict Blunt Trauma. 19th Int Symp Ballist 2001.

[5] Edwards TD, Bain ED, Cole ST, Freeney RM, Halls VA, Ivancik J, Lenhart JL, Napadensky E, Yu JH, Zheng JQ, Mrozek RA. Mechanical properties of silicone based composites as a temperature insensitive ballistic backing material for quantifying back face deformation. Forensic Science International, 285: 1-12.

[6] Sarron JC, Dannawi M, Faure A, Caillou JP, Da Cunha J, Robert R. Dynamic effects of a 9 mm missile on cadaveric skull protected by aramid, polyethylene or aluminum plate: an experimental study. J Trauma 2004;57(2):263-242.

[7] Freitas CJ, Mathis JT, Scott N, Bigger RP, MacKiewicz J. Dynamic response due to behind helmet blunt trauma measured with a human head surrogate. Int J Med Sci 2014;11(5):409-425.

[8] Rafaels KA, Cutcliffe HC, Salzar RS, Davis M, Boggess B, Bush B, Harris R, Rountree MS, Sanderson E, Campman S, Koch S, Bass CR. Injuries of the head from backface deformation of ballistic protective helmets Under Ballistic Impact, J Forensic Sci 2015;60(1):219-225.

[9] Bass CR, Bolduc M, Waclawik S. Development of a non-penetrating, 9 mm, ballistic trauma test method. Proc. Pers. Armour Syst. Symp., The Hague, The Netherlands: 2002, p. 18–22.

[10] Bass CR, Boggess B, Bush B, Davis M, Harris R, Rountree S, Campman S, Eklund J, Monacci W, Ling G, Holborow G, Sanderson E, Waclawik S. Helmet behind armor blunt trauma. Spec Conf Hum Factors Med Koblenz, Ger 2003.

[11] Aare M, Kleiven S. Evaluation of head response to ballistic helmet impacts using the finite element method. Int J Impact Eng 2007;34:596–608.

[12] Li YQ, Li XG, Gao XL. Modeling of advanced combat helmet under ballistic impact, J Appl Mech 2015;82(11).

[13] Li XG, Gao XL, Kleiven S. Behind helmet blunt trauma induced by ballistic impact: A computational model. Int J Impact Eng 2016;91:56–67.

[14] Kleiven S, Von Holst H. Consequences of reduced brain volume following impact in prediction of subdural hematoma evaluated with numerical techniques. Traffic Inj Prev 2002;3(4):303-310.

[15] NIJ Standard 0106.01 for Ballistic Helmets, US Department of Justice 1981.

[16]   Kleiven S. Predictors for traumatic brain injuries evaluated through accident reconstructions. Stapp Car Crash J 2007;51:81-114.

[17]   Tinard V, Deck C, Willinger R. New methodology for improvement of helmet performances during impacts with regards to biomechanical criteria. Mater Des 2012;37:79-88.

[18]   Post A, Oeur A, Hoshizaki B, Gilchrist MD. An examination of American football helmets using brain deformation metrics associated with concussion. Mater Des 2013;45:653-662.

[19]   Johnson KL, Chowdhury S, Lawrimore WB, Mao Y, Mehmani A, Prabhu R, Rush GA, Horstemeyer MF. Constrained topological optimization of a football helmet facemask based on brain response. Mater Des 2016;111:108-118.

[20]   Eppinger R, Sun E, Bandak F, Haffner M, Khaewpong N, Maltese M, Kuppa S, Nguyen T, Takhounts E, Tannous R, Zhang A, Saul R. Development of improved injury criteria for the assessment of advanced automotive restraint systems. NHTSA, USA 1999.

[21]   Vander Vorst M, Stuhmiller J, Ho K, Yoganandan N, Pintar F. Statistically and biomechanically based criterion for impact-induced skull fracture. Annu Proc Assoc Adv Automot Med 2003;47:363-381.

[22]   Hertz E. A note on the head injury criterion (HIC) as a predictor of the risk of skull fracture. Proc. Assoc. Adv. Automot. Med. Annu. Conf., 1993.

[23]   Sahoo D, Deck C, Yoganandan N, Willinger R. Development of skull fracture criterion based on real-world head trauma simulations using finite element head model. J Mech Behav Biomed Mater 2016;57:24-41.

[24]   Takhounts EG, Eppinger RH, Campbell JQ, Tannous RE. On the development of the SIMon finite element head model. Stapp Car Crash J 2003;47:107-133.

[25]   Ward CC, Chan M, Nahum AM. Intracranial pressure - a brain injury criterion. SAE Tech Pap 801304 1980.

[26]   Ruan J, Prasad P. The effects of skull thickness variations on human head dynamic impact responses. Stapp Car Crash J 2001;45:395-414.

[27]   Mertz HJ, Prasad P, Nusholtz GS. Head injury risk assessment for forehead impacts. SAE Pap No 960099 1996.

[28]   Prasad P, Mertz HJ. The Position of the United States Delegation to the ISO Working Group 6 on the Use of HIC in the Automotive Environment. SAE Tech Pap 1985.

[29]   Hodgson VR, Thomas LM. Breaking strength of the skull vs impact surface curvature. Final Report, 1971.

[30]   Hamouda AMS, Sohaimi RM, Zaidi AMA, Abdullah S. Materials and design issues for military helmets. Adv. Mil. Text. Pers. Equip., 2012.

[31]   Gennarelli T, Pintar FA, Yoganandan N. Biomechanical tolerances for diffuse brain injury and a hypothesis for genotypic variability in response to trauma. 47th Annu. Proc. Assoc. Adv. Automot. Med., 2003.

[32]   Margulies SS, Thibault LE. A proposed tolerance criterion for diffuse axonal injury in man. J Biomech 1992;25(8):917-923.

[33]   Bain AC, Meaney DF. Tissue-level thresholds for axonal damage in an experimental model of central nervous system white matter injury. J Biomech Eng 2000;122(6):615-622.

[34]   Bandak FA, Eppinger RH. A three-dimensional finite element analysis of the human brain under combined rotational and translational accelerations. Stapp Car Crash Conf STAPP 1994.

[35]   Pintar FA, Philippens MMGM, Zhang J, Yoganandan N. Methodology to

determine skull bone and brain responses from ballistic helmet-to-head contact loading using experiments and finite element analysis. Med Eng Phys 2013;35(11):1682-1687.

[36] El Sayed T, Mota A, Fraternali F, Ortiz M. Biomechanics of traumatic brain injury. Comput Methods Appl Mech Eng 2008;197:4692-4701.

[37] Gross AG. A new theory on the dynamics of brain concussion and brain injury. J Neurosurg 1958;15(5):548-561.

[38] Lubock P, Goldsmith W. Experimental cavitation studies in a model head-neck system. J Biomech 1980;13(12):1041-1047.

[39] Panzer MB, Myers BS, Capehart BP, Bass CR. Development of a finite element model for blast brain injury and the effects of CSF cavitation. Ann Biomed Eng 2012;40(7):1530-1544.

[40] Jenson D, Unnikrishnan VU. Energy dissipation of nanocomposite based helmets for blast-induced traumatic brain injury mitigation. Compos Struct 2015;121:211-216.

[41] Nusholtz GS, Wylie B, Glascoe LG. Cavitation/boundary effects in a simple head impact model. Aviat Space Environ Med 1995;66(7):661-667.

[42] Lozano-Minguez E, Palomar M, Infante-García D, Rupérez MJ, Giner E. Numerical comparison of mechanical models of human head under impact conditions. Int J Numer Meth Biomed Engng. 2018.

[43] Rodríguez-Millán M, Ito T, Loya JA, Olmedo A, Miguélez MH. Development of numerical model for ballistic resistance evaluation of combat helmet and experimental validation. Mater Des 2016;110:391–403.

[44] NME-2786. Requisitos técnicos para la homologación del casco de combate. Norma Militar Española, Ministerio de Defensa de España; 2013.

[45] Dassault Systèmes. Abaqus 6.12 User's Manual. 2012.

[46] Sahoo D, Deck C, Willinger R. Development and validation of an advanced anisotropic visco-hyperelastic human brain FE model. J Mech Behav Biomed Mater 2013;33:24–42.

[47] Zhou C, Khalil TB, King AI. A new model comparing impact responses of the homogeneous and inhomogeneous human brain. SAE Tech. Pap., 1995.

[48] Tse KM, Tan LB, Lee SJ, Lim SP, Lee HP. Investigation of the relationship between facial injuries and traumatic brain injuries using a realistic subject-specific finite element head model. Accid Anal Prev 2015;79:13-32.

[49] Zhang L, Yang KH, King AI. Comparison of brain responses between frontal and lateral impacts by finite element modeling. J Neurotrauma 2001;18(1):21-30.

[50] Gilchrist MD, O'Donoghue D. Simulation of the development of frontal head impact injury. Comput Mech 2000;26(3):229-235.

[51] Takhounts EG, Craig MJ, Moorhouse K, McFadden J, Hasija V. Development of brain injury criteria (BrIC). Stapp Car Crash J 2013;57:243-266.

[52] Dassault Systèmes. Section 1.2.19 VUSDFLD, Abaqus User Subroutines Reference Manual 2012.

[53] Lozano-Mínguez E, Palomar M, Infante-García D, Rupérez MJ, Giner E. Comparison of the biomechanical fracture thresholds of human head tissues through a finite element model. XXXIV Encuentro del Grup. Español Fract, Santander: 2017.

[54] Mooney M. A theory of large elastic deformation. J Appl Phys 1940;11:582–92.

[55] Rivlin RS. Large elastic deformations of isotropic materials. IV. Further Developments of the General Theory. Philos Trans R Soc London A Math Phys Eng Sci 1948;241.

[56] Yoganandan N, Pintar FA, Sances A, Walsh PR, Ewing CL, Thomas DJ, Snyder RG. Biomechanics of skull fracture. J Neurotrauma 1995;12(4):659-668.

[57] Nahum AM, Smith R, Ward CC. Intracranial pressure dynamics during head impact, SAE Tech. Pap. 770922 (1977).

[58] Tan LB, Tse KM, Lee HP, Tan VBC, Lim SP. Performance of an advanced combat helmet with different interior cushioning systems in ballistic impact: Experiments and finite element simulations. Int J Impact Eng 2012;50:99-112.

[59] Delye H, Verschueren P, Depreitere B, Verpoest I, Berckmans D, Vander Sloten J, Van Der Perre G, Goffin J. Biomechanics of frontal skull fracture. J Neurotrauma 2007;24(10):1576-1586.

[60] Macpherson BCM, Macpherson P, Jennett B. CT evidence of intracranial contusion and haematoma in relation to the presence, site and type of skull fracture. Clin Radiol 1990;42(5):321-326.

[61] Carson HJ. Brain trauma in head injuries presenting with and without concurrent skull fractures. J Forensic Leg Med 2009;16(3):115-120.

[62] Gibson TJ, Thai K. Helmet protection against basilar skull fracture. Human Impact Engineering. Canberra: 2007.

[63] Samii M, Tatagiba M. Skull base trauma: diagnosis and management. Neurol Res 2002:24(2):147-156.

[64] Ning H, Pillay S, Thattaiparthasarathy KB, Vaidya UK. Design and manufacturing of long fiber thermoplastic composite helmet insert. Compos Struct 2017;168:792-797.